STRATIGRAPHY AND STRUCTURE OF THE LATE PLEISTOCENE OLEMA CREEK FORMATION, SAN ANDREAS FAULT ZONE NORTH OF SAN FRANCISCO, CALIFORNIA

Karen Grove[1], Kevin Colson[2], Marianne Binkin[1], Robert Dull[3], Carolyn Garrison[1]

[1]Department of Geosciences, San Francisco State University, San Francisco, CA 94132
[2]Department of Geological Sciences, San Diego State University, San Diego, CA 92182
[3]Department of Geography, San Francisco State University, San Francisco, CA 94132

ABSTRACT

The Pleistocene Olema Creek Formation (OCF), consists of interbedded estuarine and alluvial sediments that were deposited on a broad coastal plain near the head of a bay similar to modern Tomales Bay. Although previously interpreted as a lacustrine deposit, recovered diatoms are those typical of estuarine environments. Arkosic sand and monotypic granitic gravel show that the Pleistocene valley was partitioned by a ridge that kept Franciscan detritus from entering the basin from the east. Paleocurrent data indicate a north-flowing drainage that requires southeastward restoration of the Salinian granitic block by at least 5.8 km. With an OCF age of 130 ka (provided by the thermoluminescence—TL—dating method), a slip rate of 45 mm/yr is obtained. A TL age of 130 ka for the Millerton Formation (exposed along the eastern edge of Tomales Bay) implies synchronous deposition of the OCF and the Millerton Formation. Deposition began during the substage 5e highstand of sea level and may have continued into successive stage 5 substages. At least 170 m of sediments were deposited in a subsiding basin that was subsequently compressed and uplifted. This evolution was a function of fault strand geometry, which changed from a diverging configuration that produced extension to a converging configuration that produced contraction. The depocenter migrated northward, and sediments are shingled in that direction; they become younger toward the head of Tomales Bay, a present site of sediment accumulation.

INTRODUCTION

The Olema Creek Formation is located within the San Andreas fault zone south of Tomales Bay, where sediments are exposed for about 3.5 km at the surface between the village of Olema to the north and Five Brooks to the south (Figs. 1 and 2). The Olema Creek Formation was first recognized and named by Galloway (1977), who briefly described the distribution, composition, age, and depositional environment of the formation. The primary sediments are granitic sand and gravel interbedded with mud that contains abundant carbonaceous material. The presence of Pleistocene freshwater diatoms in fine-grained sediments led Galloway to conclude that the Olema Creek Formation was deposited in a lacustrine environment within the San Andreas fault zone sometime during the Pleistocene Epoch.

In this paper we present the first detailed analysis of the Olema Creek Formation. We report results obtained by: measuring the sedimentary section to describe individual facies and their distribution; collecting strike and dip measurements to analyze post-depositional deformation; collecting and processing samples for paleontological analyses; and collecting samples for thermoluminescence dating of fine-grained sediments. Our data show that, in contrast to Galloway's (1977) interpretation, at least some of the fine-grained sediments were deposited within an estuarine environment, probably during the 125-ka highstand, when sea level was about 6 meters higher than at present (Chappell and Shackleton, 1986). The Olema Creek Formation is important because the sediments record events within the San Andreas fault zone, and we use our results to interpret the paleogeography of the fault valley and the style of valley deformation during the past 130 k.y.

REGIONAL GEOLOGY

The San Andreas fault (SAF) is offshore west of San Francisco and returns to land north of San Francisco at Bolinas (Fig. 1). The fault extends northwestward through the valley occupied by State Highway 1 and Tomales Bay estuary and through Bodega Bay and Bodega Head, north of where it continues offshore. In the on-land part between Bolinas and the mouth of Tomales Bay, the SAF occupies a linear valley 47 km long and

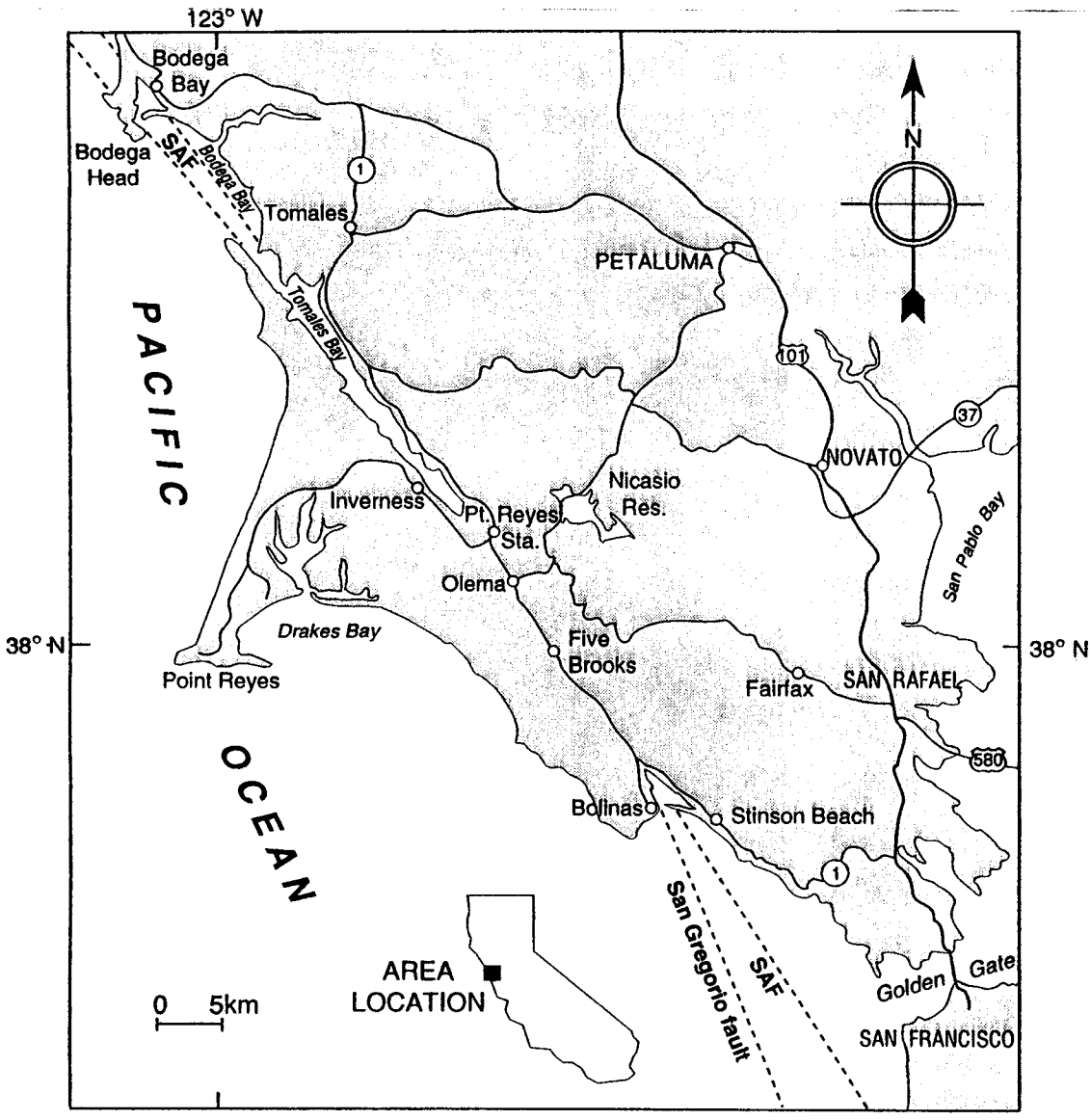

Figure 1. Location Map. Adapted from Galloway (1977). SAF=San Andreas fault.

from 0.4 to 2.0 km wide. Although the 1906 trace runs through the center of the valley, other faults appear to bound the east and west edges of the valley (called the eastern and western boundary faults by Galloway, 1977; Fig. 2). At places (e.g., near Olema), the strong topographic expression of these faults suggests recent activity, and the remarkably straight sides of Tomales Bay suggest that these faults continue to the north (Figs. 1–3). Within the valley are many fault-related landforms, including sag ponds and linear ridges.

The SAF zone, the active boundary between the North American and Pacific lithospheric plates, separates the Point Reyes Peninsula, with Cretaceous granite and older metamorphic country rocks of the Salinian terrane, to the west, from the California mainland, with graywacke sandstone and melange of the Franciscan Complex, to the east. This juxtaposition of distinctly different rock types reflects a prolonged history of strike-slip faulting that has produced about 450 km of cumulative offset since mid-Tertiary time. Dextral offset has been accommodated by at least 300 km of motion along the SAF (evidence summarized by Irwin, 1990) and about 150 km of motion along the San Gregorio fault (evidence summarized by Clark and others, 1984). The Point Reyes Peninsula is just north of the juncture between the SAF and the San Gregorio fault (Fig. 1), both part of the larger SAF system.

On the Point Reyes Peninsula, Salinian basement is overlain by a thick sequence of Tertiary marine sedimentary rocks (Clark and others, 1984) and assorted Quaternary sediments that include terrace deposits on wave-cut platforms and valley-filling alluvium (Fig. 2). Cenozoic deposits are rare on Bolinas Ridge, which consists mostly of Franciscan bedrock.

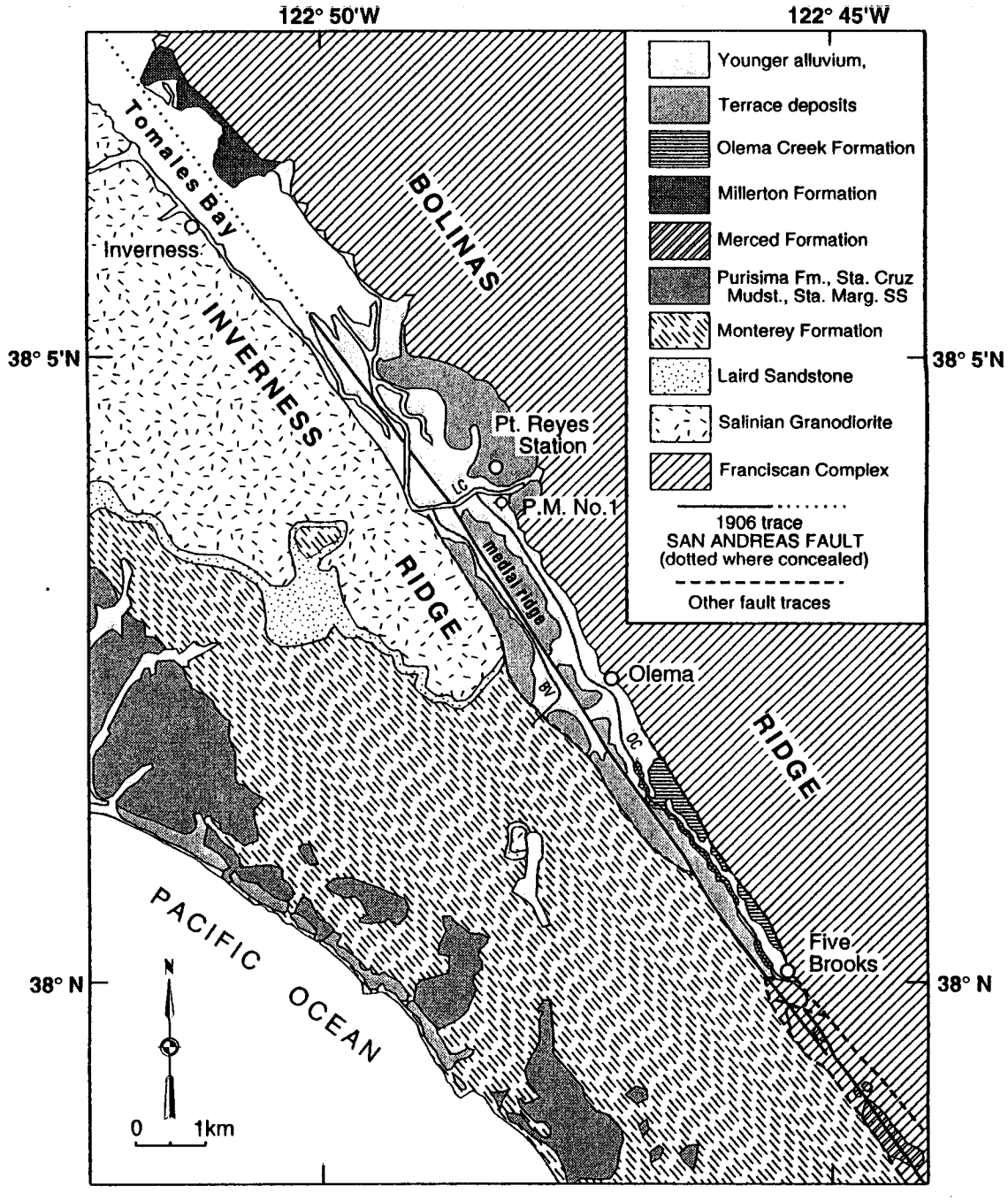

Figure 2. Regional geologic map. Adapted from Blake and others (1974), Galloway (1977) and Clark and others (1984). P.M. No.1 = dry oil well; BV = Bear Valley Creek (west side of fault valley near Olema); OC = Olema Creek (east side of fault valley near Olema). These two drainages are separated by the medial ridge. LC = Lagunitas Creek.

The SAF valley between Inverness and Bolinas Ridges (Fig. 2) contains basement rocks overlain by various Pliocene(?) to Holocene sediments. Marine sediments of the Plio(?)-Pleistocene Merced Formation that are exposed south of Five Brooks (Fig. 2) have probably been offset from the type section of the Merced Formation at the southwest edge of San Francisco, east of the SAF. The oldest nonmarine deposits in the region are of Pleistocene age. Quaternary sediments in the fault valley include the Millerton Formation, the Olema Creek Formation, terrace deposits, valley-filling alluvium, and estuarine mud associated with modern Tomales Bay. The Millerton Formation is limited in exposure to terraces along the eastern edge of Tomales Bay (Fig. 2). The formation consists of alluvial to estuarine sediments that were deposited in and around an earlier Pleistocene estuary. The Olema Creek Formation is limited in exposure to the fault valley south of Tomales Bay and

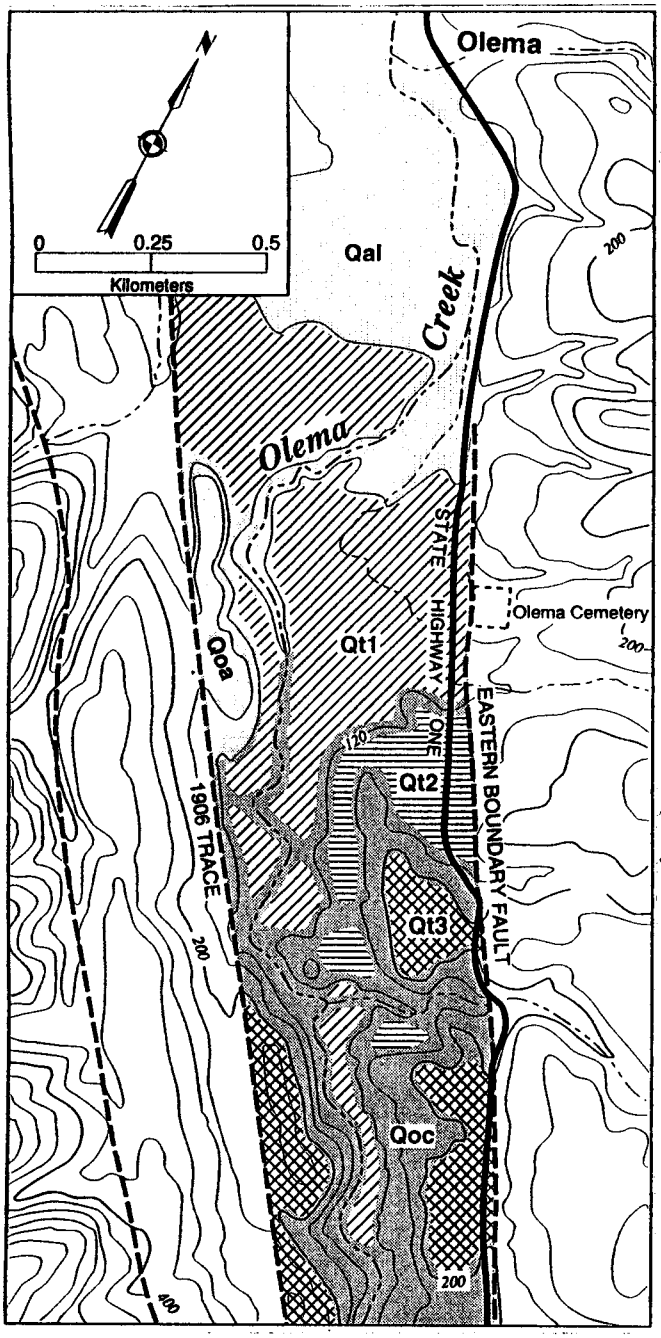

Figure 3. Topographic map of the northern end of the OCF outcrop belt showing the exposure pattern of OCF (Qoc) and overlying cut-and-fill terrace deposits. Contour interval: 40 ft. Qt1: topographically lowest (youngest) terrace; Qt2 and Qt3: topographically higher and older. Qoa (older alluvium) overlies Qoc and may be continuous with it. Both Qoc and Qoa have been incised and the incised valley is currently being filled with Qal (younger alluvium). Exposures of Qoc have so far been found only between the 1906 trace and the eastern boundary fault of the SAF system. Note that the eastern boundary fault is clearly expressed in the topography; it can be traced across the landscape by following sag ponds, saddles and linear features.

also consists of alluvial and estuarine sediments. Franciscan basement is exposed at two locations within the valley: in a belt extending from Five Brooks south toward Bolinas, and near the mouth of Tomales Bay. Basement rock types include sandstone, and melange with mafic igneous and limestone inclusions that are slices incorporated into the fault zone. Slip-rate studies based on trench wall exposures indicate that horizontal offset along the 1906 SAF trace has been 24 ± 3 mm/yr during the past 2,000 yr (Niemi and Hall, 1992).

STUDY METHODS

Investigations were concentrated in the incised valley of Olema Creek, where the Olema Creek Formation is almost continuously exposed for 2.5 km. We first determined the general structure of the formation and the stratigraphically lower beds that were the starting point for measuring and describing the sedimentary sequence. Beds were measured using a Brunton compass mounted on the end of a 1.5-meter-long Jacob's staff. Stratigraphic descriptions were used to define sedimentary facies and to interpret the environments of deposition. Clast types were evaluated to obtain information about the sediment source area.

Fine-grained samples were collected and processed to obtain paleontologic and age information. We searched for calcareous and siliceous microfossils and for pollen grains in selected organic-rich beds. Samples were also collected for dating by the thermoluminescence (TL) method; TL ages obtained from both the Olema Creek and Millerton Formations are reported in this paper.

STRUCTURAL GEOLOGY

The Olema Creek Formation (OCF) is found at the surface only as a 3.5-km-long discontinuous exposure within the confines of the SAF zone south of Olema (Fig. 2). Because of the soft nature and relative incompetence of the sediments, most of the outcrops are limited to stream banks and road cuts. The formation's east-west extent appears to be confined between the traces of the 1906 fault and the eastern boundary fault (Figs. 2–4). The eastern edge of the formation has been modified by post-depositional faulting, as it is truncated by the eastern boundary fault along the length of the outcrop belt. The western edge of the OCF is not observed because it is overlain by younger terrace deposits.

Crustal movements have subjected the OCF to compressive forces since its deposition (Fig. 4). Dips are steepest in the southern part of the outcrop belt and shallowest in the northern part. Dips also increase toward

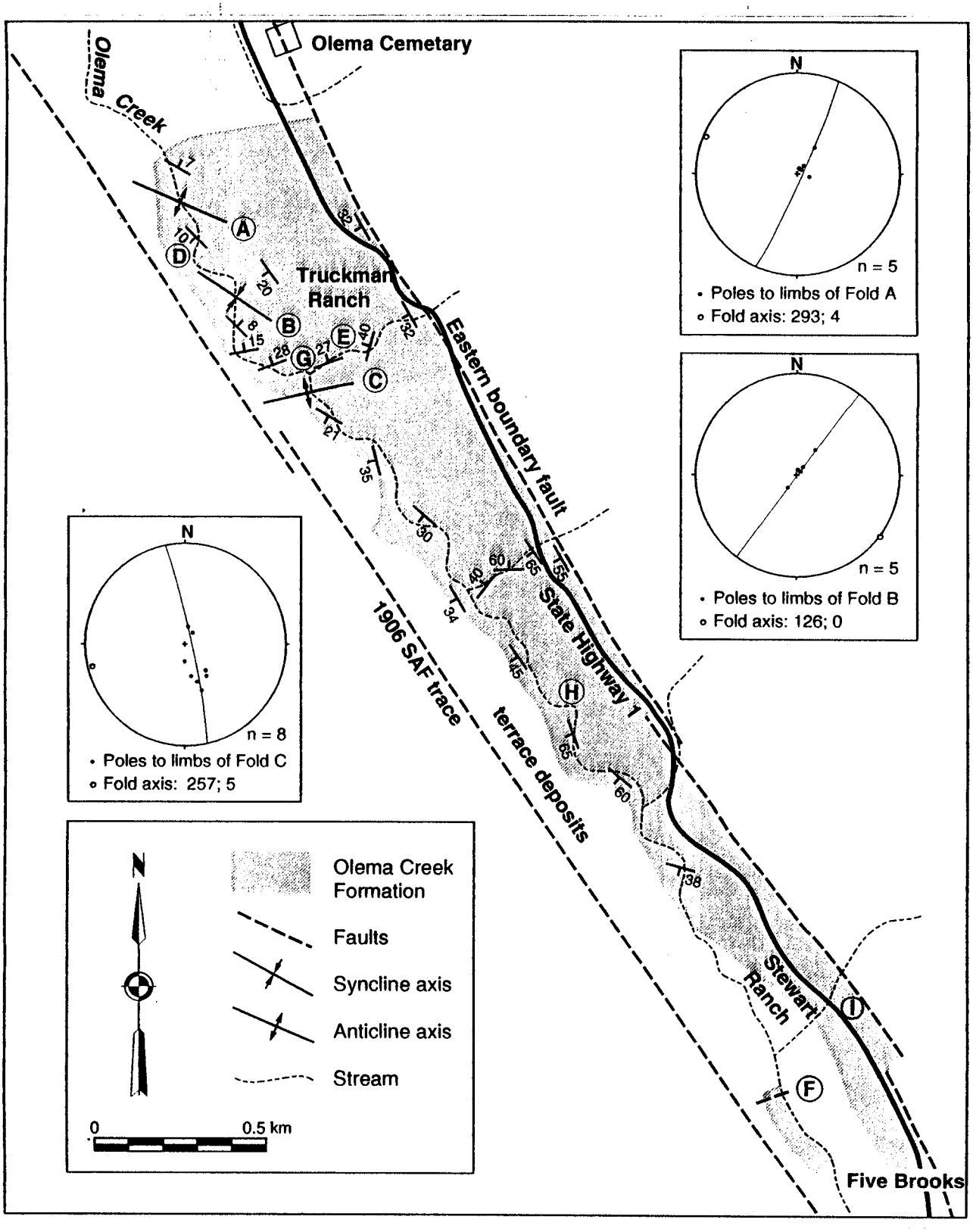

Figure 4. Outcrop map of the OCF. Fold diagrams are stereonet plots of poles to fold-limb beds. Fold axes are poles to the best-fit great circles of the limb data. The OCF is covered by younger terrace deposits throughout the outcrop belt (see Fig. 3). Localities A, B, and C are fold axes; localities D, E, and F are faults. Locality G is a pollen and diatom (O-22az) sample site. Locality H is a diatom site (O-TL1) and the thermoluminescence site. Locality I is an exposure of OCF sediments at 60-m elevation.

the eastern boundary fault, where sediments are exposed in stream cuts through overlying terrace deposits (Fig. 3). The western side of the valley is steeper and lacks stream cuts, and OCF sediments are not visible west of the cliffed cutbank of Olema Creek. Although the area west of Olema Creek was mapped by Galloway (1977) as Franciscan bedrock, Franciscan rock types are actually boulder deposits within terraces that overlie OCF sediments (Niemi, 1992).

Sediments are deformed into upright open folds with fold axes that trend west–northwest at angles of 25°–75° to the SAF trend (Fig. 4). A near-vertical fault with a N70E strike cuts the section near the south end of the outcrop belt (locality F in Fig. 4); fault and associated fracture orientations are illustrated in Fig. 5. Several small-scale thrust faults (50–100 cm long) offset beds in the central part of the outcrop belt (localities D and E in Fig. 4; Fig. 5). According to the Riedel model of simple shear, the direction of greatest compression (maximum principal stress—σ_1) should be about 45° from the primary shear trend (i.e., SAF strike; Fig. 5). Fold axis and thrust fault orientations are mostly consistent with a predicted N10E–S10W direction. By this model, F_2 could be an extensional fracture, and F_1 and F_3 could be Riedel R' shears (with expected left-lateral offset). Alternatively, with orientations predicted by the Coulomb pure shear model, F_1 could be an extensional fracture, and F_2 and F_3 could be shears. This alternative interpretation implies a compressional direction of N45E–S45W, nearly perpendicular to the SAF trend. Determining stress directions from strained features in a heterogeneous medium is always problematic but kinematic indicators from fracture surfaces could facilitate a more thorough dynamical analysis. See Aydin and Page (1984) and Sylvester (1988) for detailed discussions of structural models applied to the SAF in other parts of California.

A structural and topographic high at the southern end of the outcrop belt near Five Brooks exposes Franciscan melange with ultramafic blocks within the fault zone (Fig. 2). Available subsurface data show that the basement rock slopes generally toward the northwest. Franciscan basement was encountered at a depth of 300 m in the P.M. No. 1 well located just south of Tomales Bay (California Division of Oil and Gas, 1992; Fig. 2), and high-resolution gravity data collected along the valley between Point Reyes Station and Olema are best modeled by a northward-sloping basement surface (Quinn and Grove, 1994; Fig. 6). The OCF appears to thicken toward the northwest to fill the space overlying Franciscan basement. At the northern end of the outcrop belt, OCF sediments dip beneath younger alluvial sediments, which also thicken toward the northwest. Sediments like those of the OCF underlie younger alluvium at a depth of 35 m in the P.M. No. 1 well and extend to the basement contact

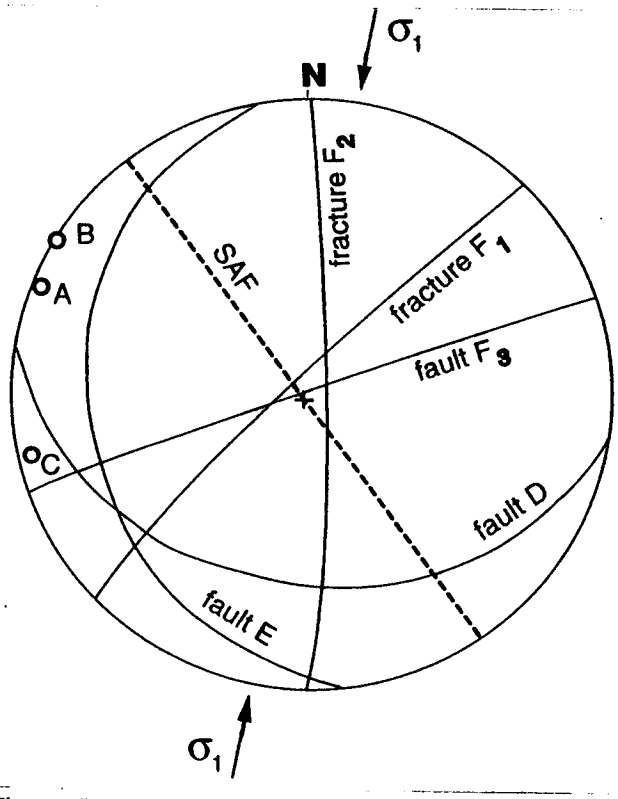

Figure 5. Stereonet plot of faults, fractures, and folds within the OCF. Locations A–F shown on Fig. 4. A, B, C = fold axes; D, E = thrust faults; F_1–F_3 = faults and fractures with uncertain movement directions. Maximum principal stress direction (σ_1) shown at 45° to the strike of the SAF (N35W), as predicted by simple shear theory. See text for analysis.

at 300 meters (California Division of Oil and Gas, 1992). Younger alluvium is, in turn, submerged beneath Tomales Bay and buried by bay mud (Daetwyler, 1996). Seismic surveys across Tomales Bay have not successfully imaged material beneath the Holocene transgressive surface (Daetwyler, 1996).

STRATIGRAPHY

Section Measurement

We chose to measure a stratigraphic section in the northern part of the outcrop belt, where a continuous sequence has strike orientations subperpendicular to the trend of Olema Creek, along the banks of which the OCF is exposed (Fig.7 contains detailed bed measurements). We measured almost 170 m of section, which is a minimum thickness.

The OCF is not observed directly overlying Franciscan basement at the surface, but it is found close to basement rocks that are exposed in the fault valley near Five Brooks. If the basin once extended further south than Five Brooks, the sedimentary record has

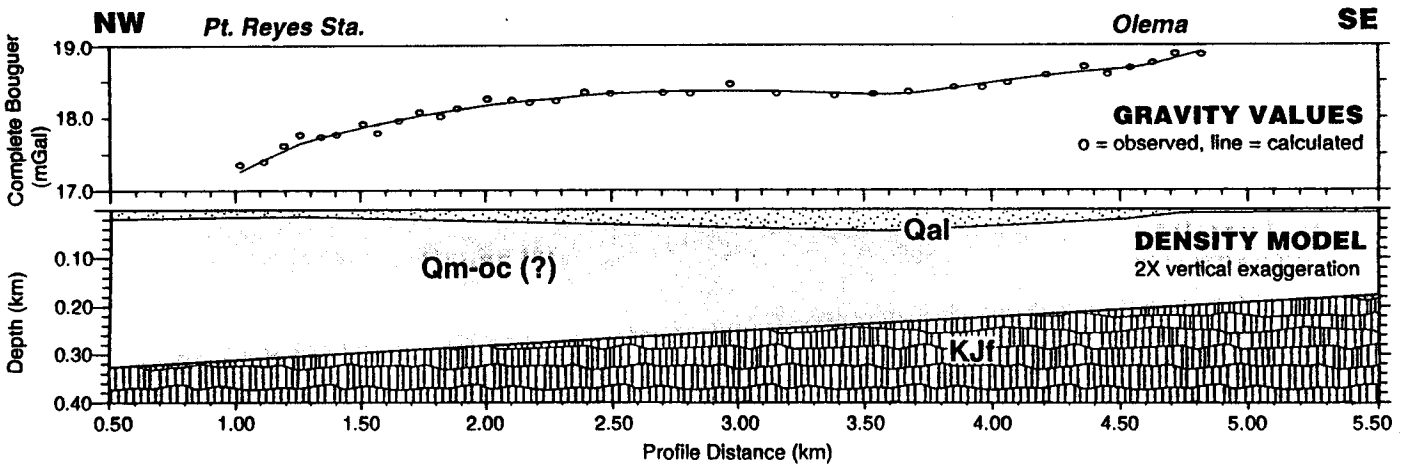

Figure 6. Gravity data from along the SAF valley between Point Reyes Station and Olema (profile azimuth is N35W). Data are best modeled by a northwest-sloping basement surface and a northwest-thickening Olema Creek Formation. Qal=valley-filling alluvium; Qm-oc(?)=Millerton and Olema Creek Formation (assumed correlative); KJf=Franciscan Complex. Data from Quinn and Grove (1994).

subsequently been removed by erosion. Throughout the southern part of the outcrop belt, OCF beds strike subparallel to the trend of Olema Creek (Fig. 4). This structure, combined with formation thinning, precluded the measurement of much section thickness in the southern outcrop area. Sediments exposed in the creek south of the fold C axis are at least partly repetitions of the lower part of the section measured further north—the oldest beds of the formation.

Excellent exposures are found in many places along the banks of Olema Creek, which in places has become deeply incised (Fig. 8). The incision by Olema Creek probably occurred during the Wisconsin glacial maximum (oxygen isotope stage 2), when sea level was 120–130 m lower than its present level (Chappell and Shackleton, 1986; Fairbanks, 1989) and axial streams carved into the floor of the fault valley (Hall and Hughes, 1980). Historic changes, such as the artificial straightening of Olema Creek, may have caused the creek to incise its floodplain an additional 1 to 4 meters (Hall and Hughes, 1980). The creek's incision has exposed OCF sediments as well as several generations of younger terrace and valley-filling alluvial deposits (Fig. 3).

Fine- and coarse-grained sediments are complexly interbedded in the OCF but there is a general trend from marine to nonmarine dominance upward in the sequence. Estuarine mud is more prevalent in the southern (older) part of the outcrop belt and alluvial sand and gravel dominates the northern (younger) part of the outcrop belt. The OCF may grade upward into the older alluvium (Qoa, Fig. 3) of Blake and others (1974), who use this designation for OCF sediments as well. Poor exposures between the northern mapped edge of the OCF and the older alluvial deposits obscure the relationship between these sedimentary units. The medial ridge (Fig. 2) consists of these older alluvial deposits, which were mapped as terrace deposits—Qt—by Galloway (1977). A 0.2-meter-thick vitric tuff found within sediments of the medial ridge (Olema tuff, Hall and Hughes, 1980) has been correlated with ash layers in the Clear Lake region and assigned a tentative age of 50–75 k.y. (Sarna-Wojcicki and others, 1988). Throughout the outcrop belt, OCF sediments are unconformably overlain by terrace gravel that fines upward to sand and soil (Fig. 9).

Sedimentary Facies

Based on composition and sedimentary structures, we divided OCF deposits into four broad sedimentary facies. Future analyses will enable us to define more specific depositional facies within these broader categories. In general, the OCF consists of sediments from the fluvially-dominated part of an estuary interbedded with sand and gravel brought to the estuary by streams and alluvial fans. The estuarine influence is lost toward the top of the sequence, which is dominated by alluvial deposits. Fine-grained overbank and backswamp deposits, with abundant carbonaceous material, are common throughout the section. The older sediments are more likely to have been deposited along the edges of tidal channels, while the younger sediments were deposited along the edges of alluvial channels. Alternations between fine- and coarse-grained deposits reflect the combined influences of subsidence along the SAF zone and climatic variations that affected the position of base level and the amount of sediment delivered to the basin.

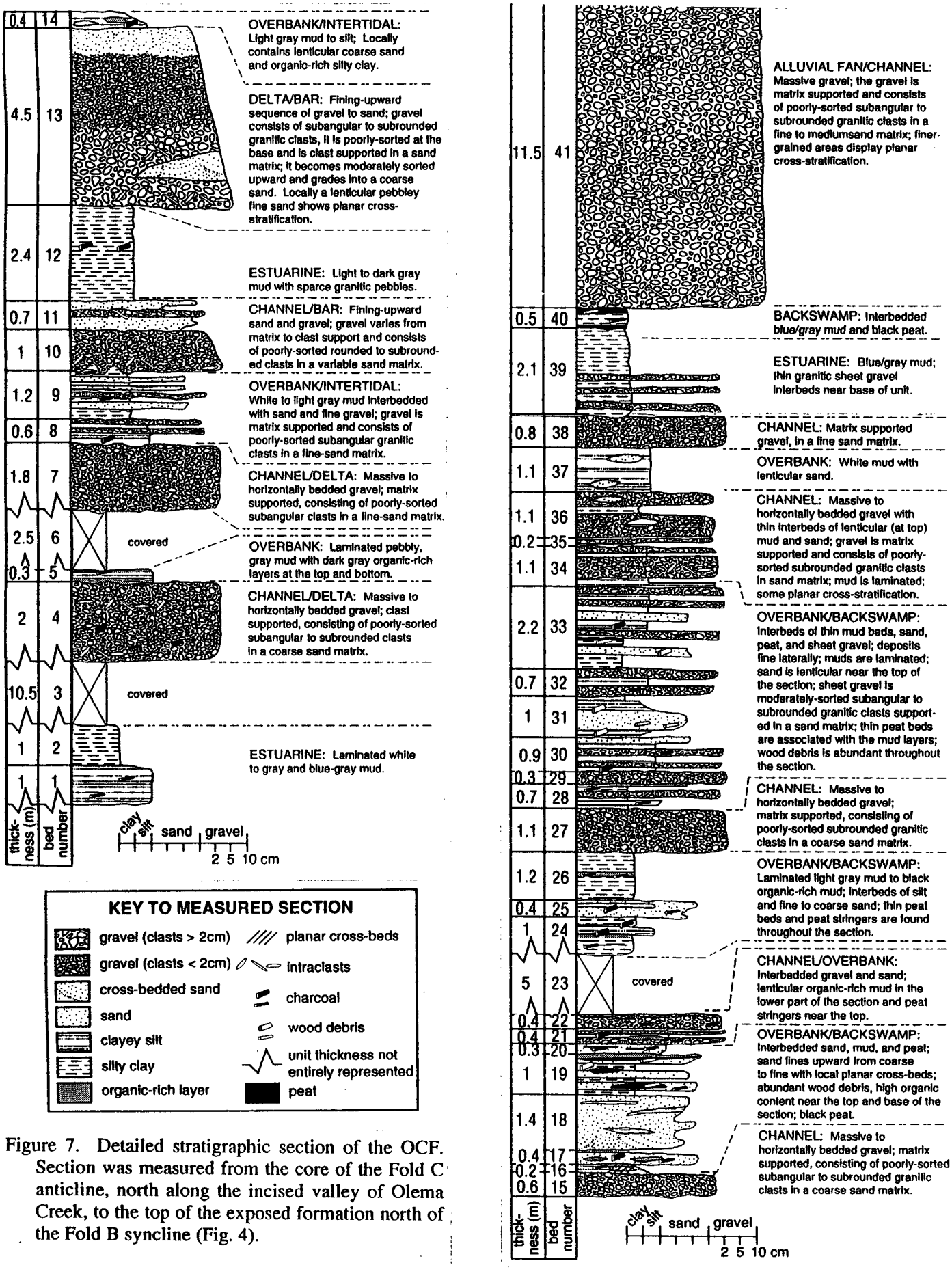

Figure 7. Detailed stratigraphic section of the OCF. Section was measured from the core of the Fold C anticline, north along the incised valley of Olema Creek, to the top of the exposed formation north of the Fold B syncline (Fig. 4).

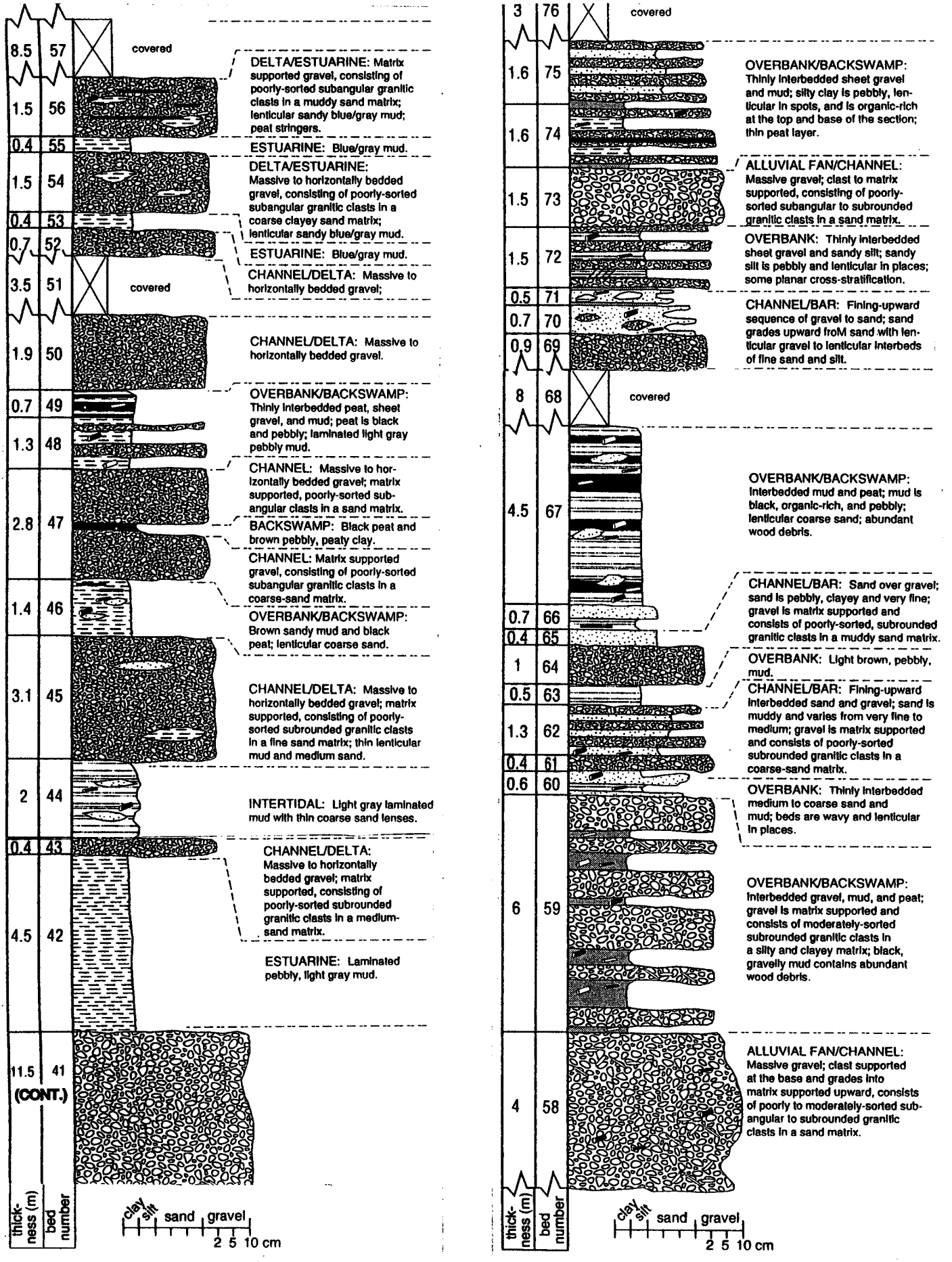
8.5 57 covered
DELTA/ESTUARINE: Matrix supported gravel, consisting of poorly-sorted subangular granitic clasts in a muddy sand matrix; lenticular sandy blue/gray mud; peat stringers.
1.5 56
0.4 55
ESTUARINE: Blue/gray mud.
1.5 54
DELTA/ESTUARINE: Massive to horizontally bedded gravel, consisting of poorly-sorted subangular granitic clasts in a coarse clayey sand matrix; lenticular sandy blue/gray mud.
0.4 53
0.7 52
ESTUARINE: Blue/gray mud.
3.5 51 covered
CHANNEL/DELTA: Massive to horizontally bedded gravel;
1.9 50
CHANNEL/DELTA: Massive to horizontally bedded gravel.
0.7 49
OVERBANK/BACKSWAMP: Thinly interbedded peat, sheet gravel, and mud; peat is black and pebbly; laminated light gray pebbly mud.
1.3 48
CHANNEL: Massive to horizontally bedded gravel; matrix supported, poorly-sorted subangular clasts in a sand matrix.
2.8 47
BACKSWAMP: Black peat and brown pebbly, peaty clay.
CHANNEL: Matrix supported gravel, consisting of poorly-sorted subangular granitic clasts in a coarse-sand matrix.
1.4 46
OVERBANK/BACKSWAMP: Brown sandy mud and black peat; lenticular coarse sand.
3.1 45
CHANNEL/DELTA: Massive to horizontally bedded gravel; matrix supported, consisting of poorly-sorted subrounded granitic clasts in a fine sand matrix; thin lenticular mud and medium sand.
2 44
INTERTIDAL: Light gray laminated mud with thin coarse sand lenses.
0.4 43
CHANNEL/DELTA: Massive to horizontally bedded gravel; matrix supported, consisting of poorly-sorted subrounded granitic clasts in a medium-sand matrix.
4.5 42
ESTUARINE: Laminated pebbly, light gray mud.
11.5 41
(CONT.)
thick-ness (m)
bed number
clay silt sand gravel
2 5 10 cm
3 76 covered
1.6 75
OVERBANK/BACKSWAMP: Thinly interbedded sheet gravel and mud; silty clay is pebbly, lenticular in spots, and is organic-rich at the top and base of the section; thin peat layer.
1.6 74
1.5 73
ALLUVIAL FAN/CHANNEL: Massive gravel; clast to matrix supported, consisting of poorly-sorted subangular to subrounded granitic clasts in a sand matrix.
1.5 72
OVERBANK: Thinly interbedded sheet gravel and sandy silt; sandy silt is pebbly and lenticular in places; some planar cross-stratification.
0.5 71
0.7 70
CHANNEL/BAR: Fining-upward sequence of gravel to sand; sand grades upward froM sand with lenticular gravel to lenticular interbeds of fine sand and silt.
0.9 69
8 68 covered
4.5 67
OVERBANK/BACKSWAMP: Interbedded mud and peat; mud is black, organic-rich, and pebbly; lenticular coarse sand; abundant wood debris.
0.7 66
CHANNEL/BAR: Sand over gravel; sand is pebbly, clayey and very fine; gravel is matrix supported and consists of poorly-sorted, subrounded granitic clasts in a muddy sand matrix.
0.4 65
1 64
OVERBANK: Light brown, pebbly, mud.
0.5 63
CHANNEL/BAR: Fining-upward interbedded sand and gravel; sand is muddy and varies from very fine to medium; gravel is matrix supported and consists of poorly-sorted subrounded granitic clasts in a coarse-sand matrix.
1.3 62
0.4 61
0.6 60
OVERBANK: Thinly interbedded medium to coarse sand and mud; beds are wavy and lenticular in places.
6 59
OVERBANK/BACKSWAMP: Interbedded gravel, mud, and peat; gravel is matrix supported and consists of moderately-sorted subrounded granitic clasts in a silty and clayey matrix; black, gravelly mud contains abundant wood debris.
4 58
ALLUVIAL FAN/CHANNEL: Massive gravel; clast supported at the base and grades into matrix supported upward, consists of poorly to moderately-sorted subangular to subrounded granitic clasts in a sand matrix.
thick-ness (m)
bed number
clay silt sand gravel
2 5 10 cm

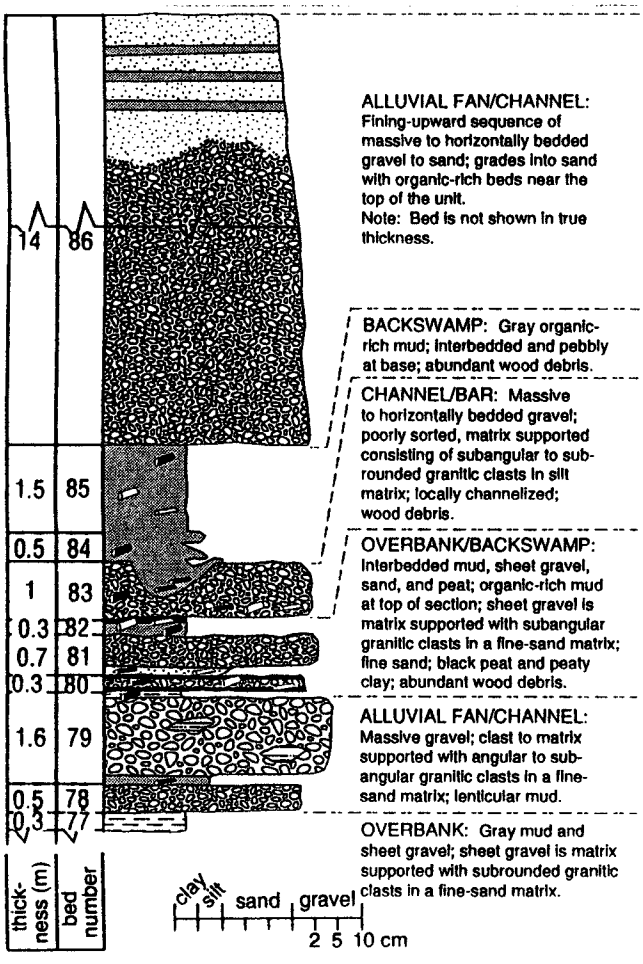

Figure 7. (Continued)

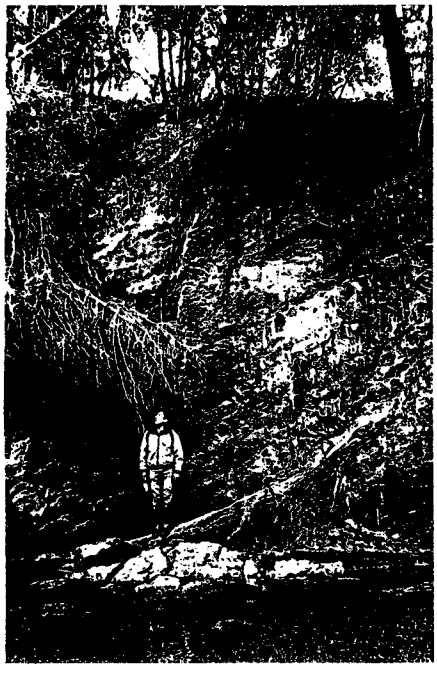

Figure 8. OCF sediments exposed on the incised banks of Olema Creek near locality G (Fig. 4). Upper meter is terrace gravel.

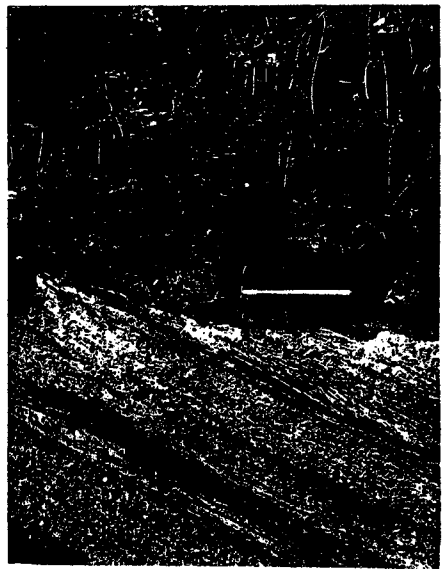

Figure 9. Thin beds of laminated and rippled mud alternating with planar pebbly sand (bed 19 of measured section—Fig. 7). OCF sediments unconformably overlain by terrace gravel that fines upward into sand and soil. Length of tool handle=15 cm.

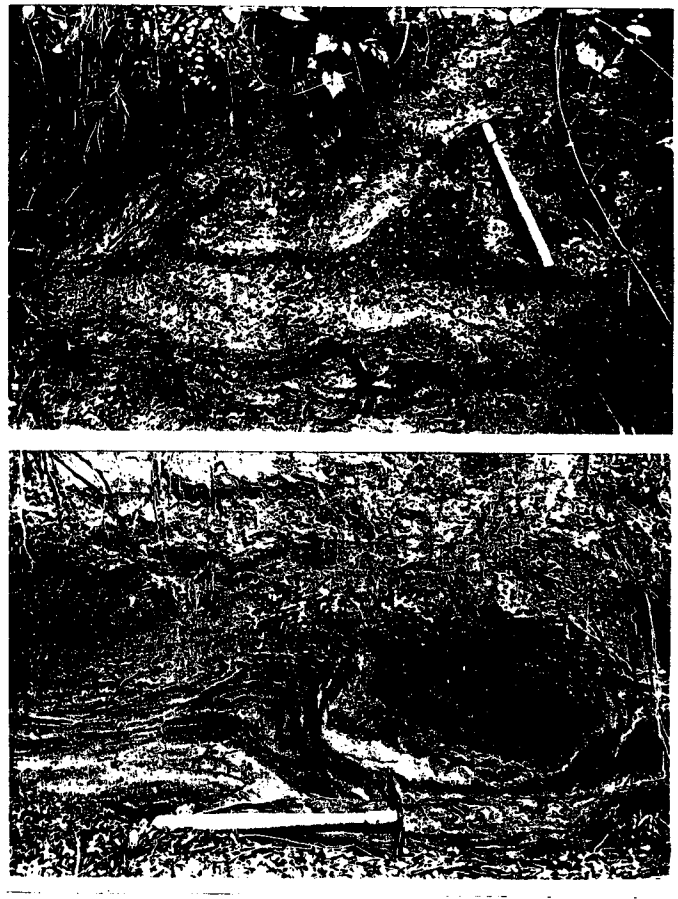

Figure 10. Top: Flame structures formed by dewatering when thick gravel layer was deposited on the black peaty layer. Bottom: soft-sediment deformation of mud probably formed during an earthquake disturbance. Length of tool handle=15 cm.

Soft-sediment deformation is common in the finer-grained sediments, where loading of overlying gravel deformed the softer underlying sediments and created flame structures (Fig. 10). Soft-sediment deformation is also present in some mud beds not overlain by gravel. These show evidence of intense, small-scale internal folding that may be linked to earthquakes in the SAF zone (Fig. 10).

Open Estuary Facies

Thick beds of massive to horizontally-laminated mud (ranging from silty or sandy clay to clayey silt) are interpreted as estuarine deposits. The sediments have a bluish-grey color when freshly exposed in outcrop, but change to a grayish olive to greenish gray color when removed from the outcrop and dried. These colors reflect deposition within a reducing environment with a high clay content. Although no macrofossils have been recovered, laminations are probably absent from the massive beds because of pervasive bioturbation. For example, Anima and others' (1988) sampling of modern sediments in Tomales Bay showed that bay mud was extensively bioturbated just 9 months after deposition. Some of the contacts between underlying or overlying coarser-grained layers are gradational where the coarser sediments have been irregularly mixed with the mud, also probably by bioturbation. Other bed contacts are very sharp. The mud beds of this facies were probably deposited in subtidal to intertidal estuarine flats.

Diatoms recovered from layers of this sedimentary facies led Galloway (1977) to interpret the OCF as a lacustrine deposit, but we recovered diatoms that are found in marine and brackish as well as freshwater environments (Table 1). For example, *Thalassionema nitzchioides* is a planktonic form that is "abundant and widespread in the Yerba Buena mud" (Sangamon-aged mud of San Francisco Bay; Laws, 1988) and *Navicula cryptocephala* is a form "common...in intertidal mud flats and marsh sediments of present day, Albany mud flats" (around San Francisco Bay; Laws, 1988). Sample O-22az, which has poor preservation and abundant fragments, was collected from the base of the measured section (lateral equivalent of covered bed 23 in Fig. 7, locality G in Fig. 4). Sample O-TL1, which has good preservation and abundant diatoms, was collected from a bed located south of the measured section, at the site sampled for thermoluminescence dating (locality H in Fig. 4).

Diatoms from Galloway's (1977) samples may have been misidentified, at least in part, because of poor information about brackish-water assemblages (P. Kociolek, pers. comm., 1993). G. D. Hanna, who was an open-marine specialist at the California Academy of Sciences (CAS), identified the diatoms. Unfortunately, Galloway's specimens and information about the locations from which the samples were collected have been lost from the CAS collections. Recent work by Laws (1988) on Sangamon to Recent diatoms from San Francisco Bay has provided an improved understanding of west coast brackish-water assemblages since Galloway's (1977) original interpretation.

DIATOM SPECIES	SALINITY	O-22	O-TL
Aulacosira granulata	freshwater		XX
Cocconeis placentula	indifferent		XX
Coscinodiscus sp.	marine	X	X
Cyclotella striata	brackish-marine		XXX
Cymbella triangulum	freshwater		XX
Epithema turgida	indifferent		XX
Gomphonema parvulum	freshwater		XX
Navicula cryptocephala	fresh-brackish		XX
Thalassionema nitzchioides	marine	XX	X

Table 1. Diatom species from the OCF (sample locations in Fig. 4). X=rare; XX=common; XXX=abundant. Samples identified with reference to Laws (1988). See Laws (1988) for salinity references.

Overbank/Backswamp/Intertidal Facies

Numerous subenvironments are lumped together into this facies because the deposits are intimately interbedded and are all laminated to thin, laterally continuous beds that were deposited in environments characterized by persistently changing energy levels. These sediments were deposited near the head of an estuary, where small variations in base level could produce rapid changes in the relative amounts of fluvial and tidal influence. Even with a stable base level, locations near the heads of estuaries have a strong fluvial influence, with lower water salinity and attenuated tidal flow producing a net seaward-directed flow throughout the water column (for a description of estuary parts—from fluvial- to marine-dominated—see Nichols and Biggs, 1985). A good example of this facies is beds 16–22 in the measured section (Fig. 7; photograph in Fig. 9). Thin beds of silt and clay contain planar to rippled internal laminations that alternate with black, organic-rich peat layers. Depending on the amount of carbonaceous material, and the clay:silt ratio, colors range from white to medium light gray to greenish gray or brownish gray. Some layers are yellowish gray to brown and others contain bright yellow sulfurous material. These colors suggest, like the open estuary facies, a reducing environment. Preservation of abundant organic material supports the low-oxygen interpretation.

Fine-grained sediments of this facies were deposited in the overbank areas adjacent to fluvial or tidal channels when the creeks flooded their banks during storms or during flood tides. Some beds contain alternating planar laminations of mud and silt–sand layers that probably reflect the alternating bedload and suspension sedimentation that occurs during changing energy levels of a tidal cycle (Fig. 11). Ripple laminations with mud drapes are other evidence of probable tidal bedding (Klein, 1985). Some of these beds grade into open-estuary mud, suggesting deposition within tidal flats or other shallow-water environments on the edge of an estuary (tidal-wetland lithofacies of Fletcher and others, 1990).

Peat beds contain a large variety of plant material, including leaves, pine cones, roots, and branches. At one location, near the axis of the fold B syncline, a whole tree trunk with branched roots occurs in growth position in muddy sediments (Fig. 12). We have not yet identified the pieces of macroflora, but we have analyzed two samples of fine-grained sediment for their pollen content (Table 2). One sample is from a brownish-gray laminated mud within bed 19 (Fig. 7) and the other is from one of the beds that contains estuarine diatoms (sample O-22az). The abundance of aquatic plants (e.g. Cyperaceae and *Potamogentan* types) is consistent with a swamp interpretation. Riparian plants (e.g., *Alnus* and *Salix* types) also prefer a wet environment; these plants (alders and willows) are today observed along the edges of the tidal wetlands and creeks near Tomales Bay. Peat beds are interpreted as backswamp, standing-water deposits. Further analyses of plant material in peat beds should aid our interpretation of these sediments as either fresh- or salt-water marsh deposits. Some of the thicker peat beds contain many large, woody pieces; these trees were probably growing in a fresh-water pond.

Other nonmarine influences are shown by intercalated beds of sand and fine gravel up to 20-cm thick. Most of these beds contain crude planar layers that are interpreted as laterally continuous sheet flows. These layers are attributed to large storm events that caused fluvial or tidal creeks to flood their banks and deposit sheet gravel in the overbank areas. Sand and/or gravel sand waves that are draped with mud (Fig. 13) show evidence of alternating energy levels.

Channel Fill/Bar/Delta Facies

This coarse-grained facies includes medium-sand to cobble-sized sediment that is planar or cross bedded. Some beds contain imbricated gravel clasts or mud intraclasts. Beds with abundant sand, cross-stratification, and distinct fining-upward sequences are interpreted as point bars that accumulated in creek channels. Cross beds

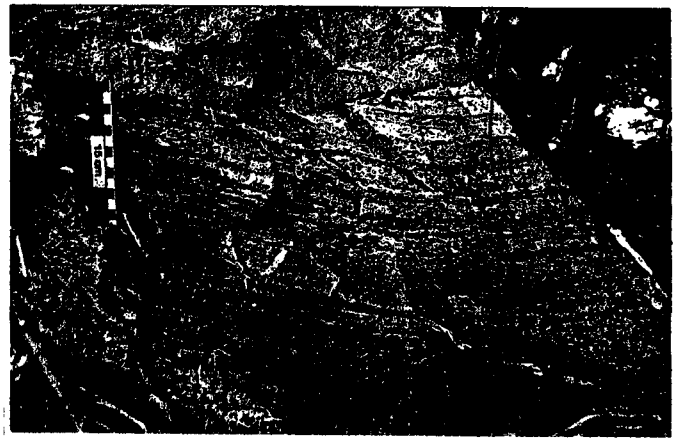

Figure 11. Laminated interbedded mud and silt to fine sand that is probable tidal bedding.

Figure 12. Tree trunk in growth position with intact roots (flat-lying bed in the core of the Fold B syncline—Fig. 4). Length of tool handle=15 cm.

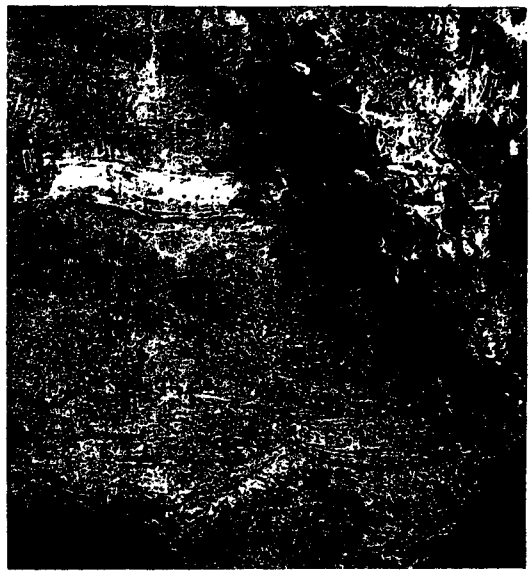

Figure 13. Five-cm-high sand wave draped with mud laminations, overlain by fining-upward pebbly sand and laminated white to light-gray mud (cm-scale on left side of mud layer), overlain by pebbly sand.

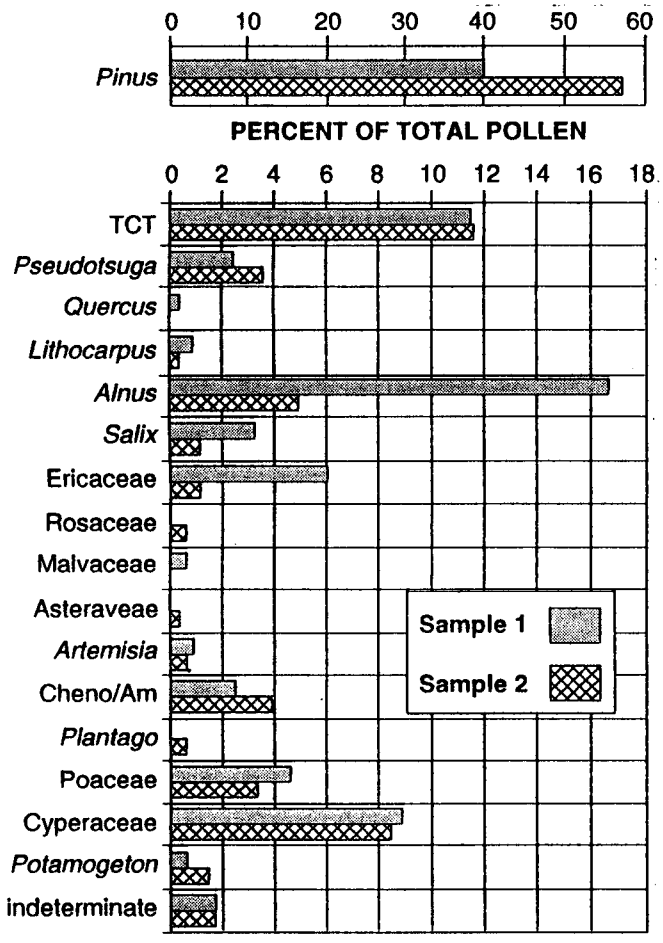

Table 2. Pollen diagram from two beds at locality G (Fig. 4). About 400 grains were identified in each sample. Sample 1 is from laminated, brownish-grey mud that is interbedded with white to grey mud, black peat, and thin sheet gravel (overbank facies). Sample 2 is from massive to laminated blue-gray mud (open estuary facies). Non-italicized types are family level. TCT is three families of trees—Taxaceae, Cupressaceae, and Taxodiaceae; *Pinus*, TCT, and *Pseudotsuga* (Douglas fir) are all conifers. *Alnus* (alder) and *Salix* (willow) are riparian trees that need a high water table. Cyperaceae and *Potamogeton* are aquatic plants that also have high water requirements. Other pollen types are from a wide variety of plants, but they are primarily grasses, shrubs, and herbs.

of gravel, up to 50-cm thick, are interpreted as the deposits of migrating bars within fluvial channels. Measurements of cross beds within this facies indicate a northerly direction of flow, like that of modern-day Olema Creek (Figs. 14 and 15). Some of the laterally continuous, thinner beds may have been deposited in broad, shallow channels. The streams that deposited these sediments were part of an axial drainage system that paralleled the SAF system as the valley does today.

Some of the sediments in this facies are deltaic deposits from the mouths of creeks that fed into the estuarine environment. For example, after the 1982 storm, small deltas were formed at the mouth of nearly every creek that feeds into Tomales Bay (Anima and others, 1988). Similarly, Nichols and Biggs (1985) described the tendency of rivers to build a deltaic sediment mass in an estuary head (estuarine fluvial zone), where the river debouches into the open estuary to form a delta-front shoal. The geometry of estuarine mud onlapping sandy gravel beds that taper seaward supports this deltaic interpretation (Fig. 16).

Figure 14. Cross-bedded sand and gravel layers. Sand bed in middle of sequence=10 cm high.

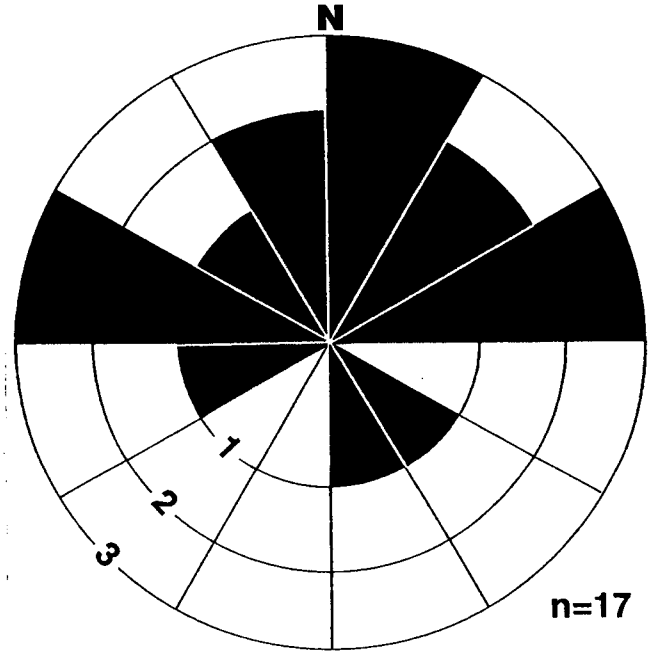

Figure 15. Paleocurrent directions measured from medium-scale cross beds in channel sand and gravel of the OCF.

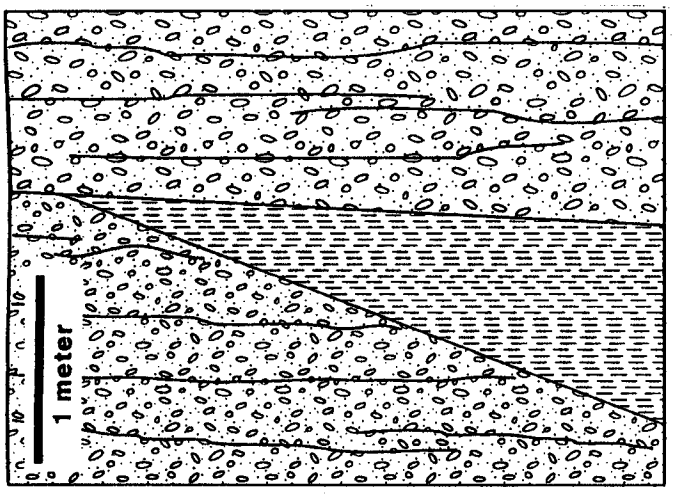

Figure 16. Diagram of vertical sequence where estuarine gray mud onlaps a sand and gravel bed (probable delta lobe) and is overlapped by more sand–gravel. The lower bed tapers (thins) toward the north (seaward) and the mud thickens northward.

Alluvial Fan Facies

The coarsest-grained and thickest of the OCF beds show little to no stratification and contain poorly-sorted angular clasts. These massive beds are interpreted as alluvial-fan deposits derived from the ridge west of the valley (transverse drainage). Sediment was transported by sediment gravity flows (e.g., debris flows) down the slopes of steep-sided fan surfaces and into the valley.

Sediment Analysis

Sand- and gravel-sized sediment occurs throughout the OCF. The gravel is found in beds ranging in thickness from a few cm to many m. These beds are composed of subangular to subrounded clasts in a sand matrix, with either clast or matrix support. Both sand and gravel in the formation are weakly cemented with clay or iron oxide. The gravel is mostly poorly- to moderately-sorted with clast sizes ranging from 1–10 cm, and with most clasts measuring about 2 cm in diameter. They are predominately granitic in composition, with no gravel bed containing more than 15% nongranitic clasts. The nongranitic gravel-sized clasts are schists, intraformational mud, and rare Franciscan graywacke. OCF sediments were derived primarily from the western side of the fault valley, where granitic basement of the Salinian terrane is exposed. Sedimentary rocks of the Monterey Formation are presently located west of the OCF outcrop belt, however, and offset along the SAF has moved granitic basement rocks north of the outcrop belt since OCF deposition.

The finer-grained components of the formation are sand, silt, clay, and organic material. The sand and silt are arkosic, composed primarily of quartz and feldspar grains derived from granitic basement rock. The organic material consists of peat and plant debris, including pine cones, leaves, roots, branches, and tree trunks and branches, as well as numerous small pieces we have not yet identified. Some of the fine-grained beds are white in color and look very much like tuffs. Microscopic investigation of these beds, however, revealed no glassy material; nor do they contain diatoms. We have concluded that these beds are composed of arkosic silt with feldspars that were heavily weathered to clays in the source area before being deposited within the valley below.

An unusual mineral found within several beds of estuarine mud is apparently vivianite (C. Bickel, pers. comm., 1995). This mineral has a white color that changes to a bright, cobalt blue color when removed from the outcrop and dried. Its habit is a reniform crust that occurs throughout the sediment in patchy splotches. The refractive index of this mineral matches that of vivianite, a rare hydrated iron phosphate that darkens when exposed to air (C. Bickel, pers. comm., 1995).

Thermoluminescence and Radiocarbon Age Data

The only age data previously obtained from the OCF were radiocarbon measurements of fossil wood. Galloway (1977) reported an age of 38,700 ± 2000 yr. B.P., but subsequent analyses by Niemi (1992) has shown that wood within the formation is >41,000 yr. We submitted wood pieces from the unconformity between the OCF and overlying terrace deposits to Beta Analytic Inc. for radiocarbon analysis. Our results also indicate wood that is >47,000 yr old, beyond the range of radiocarbon resolution.

One bed of blue-grey estuarine mud was sampled for dating by the thermoluminescence (TL) method by G.W. Berger (locality H on Fig. 4), and analyzed in his TL laboratory at Western Washington University. This sample yielded a TL age of 132 ± 28 ka. The large error resulted from poor behavior of the sample under laboratory conditions and insufficient preheating of the sample (G.W. Berger, pers. comm., 1994). Nevertheless, the age range is consistent with deposition during oxygen isotope substage 5e, a time when sea level was about 6 meters higher than the present level (Chappell and Shackleton, 1986; Fig. 17) and marine water could have penetrated further south into the fault valley than it does now. A sample collected from the Millerton Formation along the northeastern edge of Tomales Bay behaved better under laboratory conditions and yielded a TL age of 134 ± 12 ka (G.W. Berger, pers. comm, 1994). This

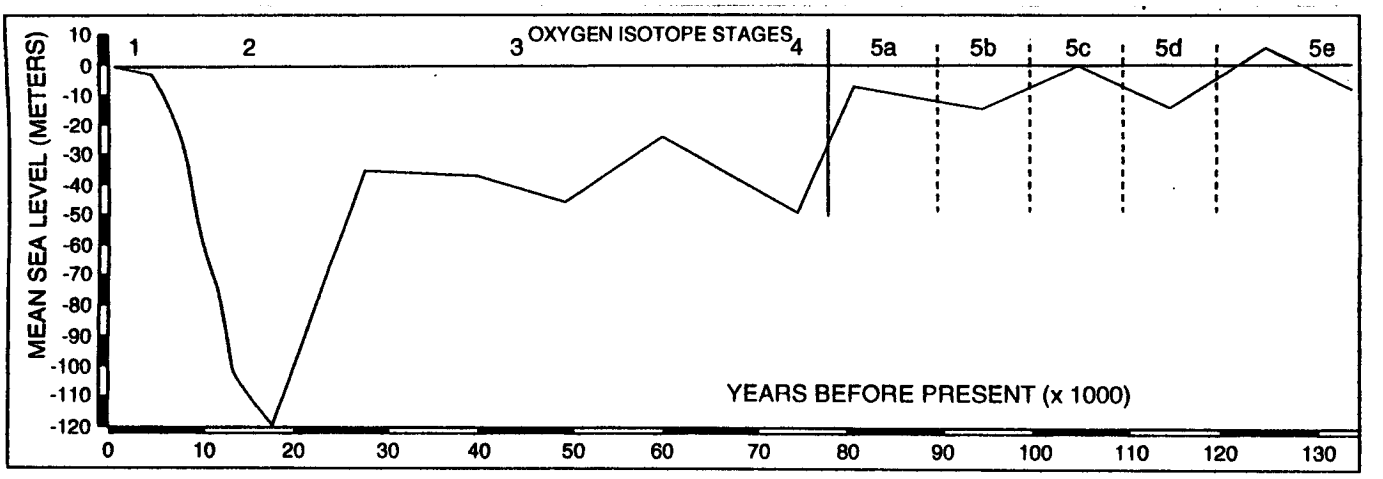

Figure 17. Late Quaternary sea-level curve from glacio-eustatic records. Diagram adapted from Toscano (1992). Data from Bloom and Yonekura (1985), Fairbanks (1989), and Li and others (1989).

age is consistent with a previously obtained aminostratigraphic age (Kennedy and others, 1982) and suggests that at least parts of the Olema Creek and Millerton Formations were deposited simultaneously during the 5e substage highstand of sea level.

Modern Analog

A modern analog for the depositional environment of OCF sediments is the head of Tomales Bay, at least prior to diking of the marsh lands and filling for agricultural use. Estuarine sediments here interfinger with alluvial sediments on a broad coastal plain, where creeks transport sediment northward along the axis of the valley, and alluvial fans accumulate sediments in valleys that are perpendicular to the axial valley. Hollows (gully-like valleys) also accumulate sediment which is evacuated during major storms and transported in debris flows to the bay (Reneau and others, 1990). During storms, sand and gravel deltas form at the mouths of creeks that also feed into the bay (Anima and others, 1988; Fig. 18).

Numerous marshes and swampy areas occur around the head of Tomales Bay. For example, a large freshwater marsh lies along the 1906 SAF trace near where Bear Valley Creek empties into Lagunitas Creek (Fig. 2). This marsh may have had some tidal influence prior to construction of the levees that separated the marsh from the estuary. In the broad, flat part of the valley between Olema and the head of Tomales Bay (Fig. 2), low areas are often sites of standing water (Fig. 19).

The head of Tomales Bay lies adjacent to Salinian granite outcrops (Fig. 2) that supply sediment into the modern valley as they did to the OCF basin. The granitic rock weathers readily to grus, which forms alluvial fans along the western edge of the valley (e.g., those mapped by Hall and Hughes, 1980). A medial ridge partitions the axial drainage into two parts that reflect the different rock types on each side of the fault valley (Fig. 19). Gravel in Bear Valley Creek (west side of the medial ridge) contains mostly granitic and Monterey Formation clasts from the Salinian terrane to the west and gravel in Olema Creek (east side of the medial ridge) contains mostly sandstone and greenstone from the Franciscan Complex to the east (Niemi, 1992).

Sediments in the southern half of Tomales Bay estuary are massive to laminated silty clays to clayey silts with thin layers of sand and/or gravel near the margins of the estuary (Daetwyler, 1966). Core data are not available from the marshy area at the head of Tomales Bay, where coarser-grained sediment supplied by creeks must be interbedded with estuarine mud, as it is in the OCF. Following the great 1906 San Francisco earthquake, numerous features, such as crater-like depressions and undulating ridges and troughs on the tidal flats, were observed around the edge of Tomales Bay (Lawson, 1908). These features would produce soft-sediment deformation similar to the disrupted beds found in OCF sediments. The presence of littoral sediments at 300-m depth just south of Tomales Bay (in P.M. No. 1 well, Fig. 2), shows that the area around the head of the bay has been subsiding during the past 100,000 years.

Figure 18. Head of Tomales Bay on the west side of the bay 1–2 km southeast of Inverness (Fig. 2); view toward the bay—north). Water on the right is tidal channel connecting to the bay; central vegetated area is tidal marsh with standing water, and light area on the left is granitic grus that has entered the marsh by streams and debris flows from Inverness Ridge to the west (left of photo). Alders and other riparian plants grow along the edge of the tidal marsh.

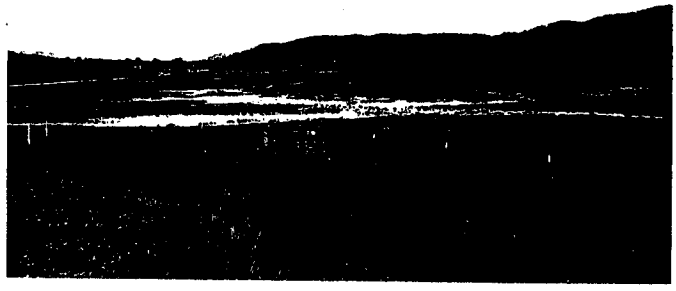

Figure 19. View of the SAF valley looking south. Standing water in a broad, flat part of the valley south of Tomales Bay. View is toward Olema, with State Highway 1 on the left, and the medial ridge on the right (see Fig. 2). Trees along the base of the medial ridge mark the present location of Olema Creek. At this location the medial ridge partitions the axial drainage into two parts—Olema Creek drains the east side and Bear Valley Creek drains the west side.

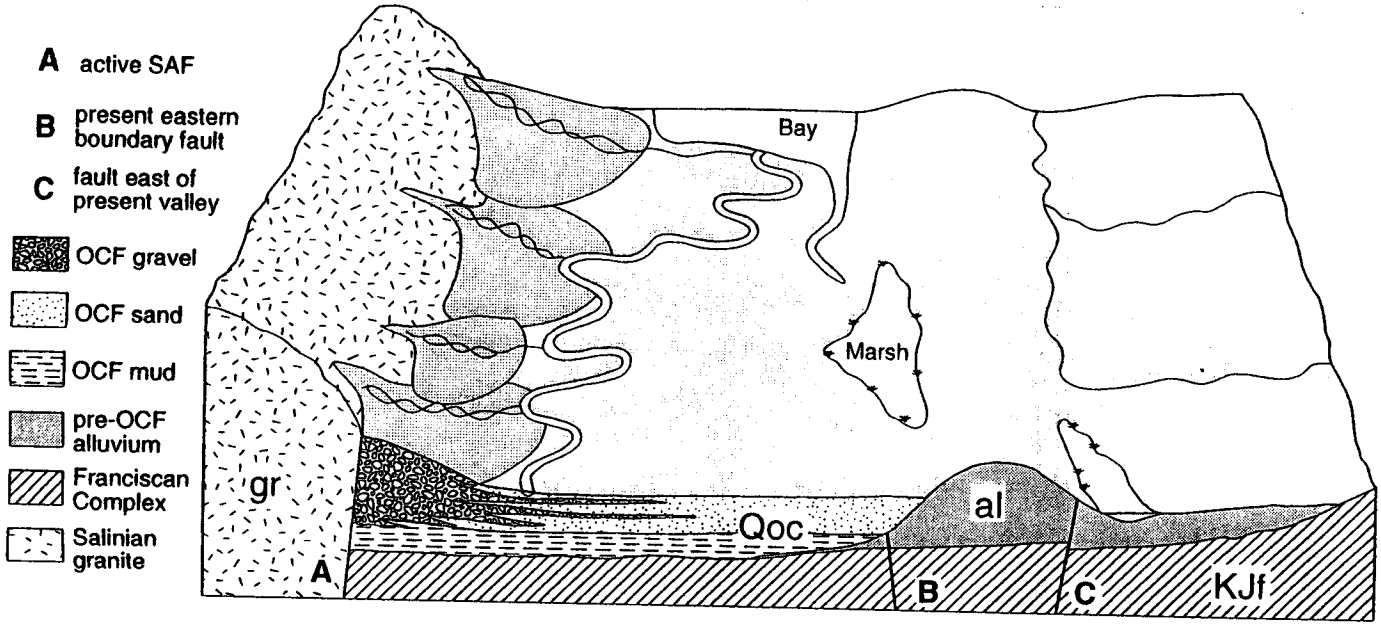

Figure 20. Paleogeographic reconstruction of the SAF valley during deposition of the OCF. View is to the northwest, toward the ancestral bay. Franciscan detritus (KJf) is separated from the OCF depocenter by a ridge composed of older valley-filling alluvium (since removed by uplift and erosion east of the eastern boundary fault). The alluvium may have been interbedded with older bay mud from previous sea level highstands. Granitic highlands to the west (now moved north of the site by SAF motions) supplied sediment to the OCF basin.

IMPLICATIONS FOR SAN ANDREAS FAULT VALLEY EVOLUTION

Paleogeography

Within the outcrop belt of the OCF, the modern Olema Creek is confined to meandering within a narrow incised valley rarely wider than 100 meters. When OCF sediments were deposited, however, creeks meandered within a wider floodplain, more like the broad coastal plain further north near the head of Tomales Bay (Fig. 2). OCF deposits extend the width of the SAF zone, and their lateral extent could have been even greater than what is presently visible. To the east, deposits are truncated by the eastern-boundary fault, and to the west, they are covered by terrace deposits.

The OCF basin extended in length at least from Five Brooks to Olema. It may have continued south of Five Brooks, but if so, no sediments are preserved. OCF-like sediments are buried in the subsurface near the head of Tomales Bay and the formation is at least partially correlative with the Millerton Formation exposed further north along the eastern shore of the bay.

Preserved sediments of the OCF were deposited within rivers and alluvial fans and the river-dominated part of an estuary, where tidal flow was attenuated and seaward (northwestward) river flow prevailed. Alluvial fans accumulated sediment at the base of a granitic outcrop belt to be swept into the estuary during storms and to be reworked by axial creeks (Fig. 20). As the Pleistocene stream encountered the gravelly fans of granite, they reworked these sediments to form channel-fill and bar deposits. The stream became braided when the sediment load of grus exceeded the capacity of the stream. Crudely upward-fining sequences and abundant fine-grained deposits within the OCF suggest at least some deposition within a meandering channel with broad areas of interchannel overbank (floodplain) deposition. The numerous organic-rich beds were deposited in oxygen-deficient backswamps and ponds. In addition to the overbank areas between channels typically encountered in a river system, low areas were formed as sag ponds or marshes developed along the SAF zone (Fig. 20). Episodic subsidence during earthquakes and sea-level fluctuations caused periodic inundation of the valley by marine water to create an estuarine environment.

Sediments in modern Olema Creek contain a mixture of clast types derived from both sides of the fault valley, and Franciscan clast types dominate the gravel population (Niemi, 1992). During OCF time, however, sediments were derived primarily from the west, where granitic basement of the Salinian terrane lay adjacent to the ancestral SAF valley. At this time, the large granite outcrop now located west of the 1906 SAF trace and the town of Inverness (Fig. 2) was adjacent to the Pleistocene depositional basin.

The lack of Franciscan-type clasts within the OCF suggests that either (1) a geographic barrier separated the Franciscan source area from the depositional basin; or (2) the Franciscan basement was poorly exposed or characterized by a landscape of relatively low relief at the time of OCF deposition. Terraces that bevel the western slope of Bolinas Ridge have unknown ages, but they indicate a ridge that has been rising in elevation for some time. It is likely, therefore, that a ridge within the valley acted as a barrier to sediments supplied from the east, much as the medial ridge today partitions the fault valley into separate drainages (Fig. 20). Unlike OCF streams, modern Bear Valley Creek (west of the medial ridge) has only a narrow floodplain, but like OCF streams, its sediments are derived almost exclusively from Inverness Ridge to the west (Niemi, 1992; Fig. 2). Additionally, Bolinas Ridge has been rising relative to the valley floor, and at 125 ka it may have been topographically lower than it is now. The timing of uplift, however, awaits new age information for the terraces.

Deposition of OCF sediments began about 130 ka, when marine waters began to flood the fault valley during a sea level highstand about 6 m higher than the present level (oxygen isotope substage 5e; Fig. 17). The duration of OCF sedimentation, however, is uncertain. Age constraints are a thermoluminescence date of about 130 ka from near the base of the OCF and a tuff with a probable 50–75 ka age from overlying alluvium (Qoa). Alternating estuarine and alluvial sediments throughout the more than 170-m-thick formation imply persistent subsidence followed by periods of basin filling, and sea-level fluctuations, as well as tectonic subsidence, must have affected these processes. There is evidence that stage 5 sea level remained high for some time. For example, Sherman and others (1993) showed evidence for two sea-level highstands just within the 5e substage (at about 120 ka and 133 ka), and Li and others (1989) determined that sea level remained above -15 m MSL (mean sea level) for the entire interval of 133 to 110 ka. Subsequent stage 5 substages (e.g., the highstands of substages 5c and 5a and the lowstands of substages 5d and 5b, see Fig. 17) could have caused some of the variations between alluvial and estuarine environments that are observed in the OCF. Toscano (1992) provided an example of substage identification based on littoral sediments found along the U.S. east coast. The extensive alluviation that occurred in the SAF valley toward the end of OCF deposition, and that apparently continued for some time prior to the Wisconsin incision (isotope stage 2), could have occurred as sea level was lowering from stage 5 levels. For example, Kelsey and Bockheim

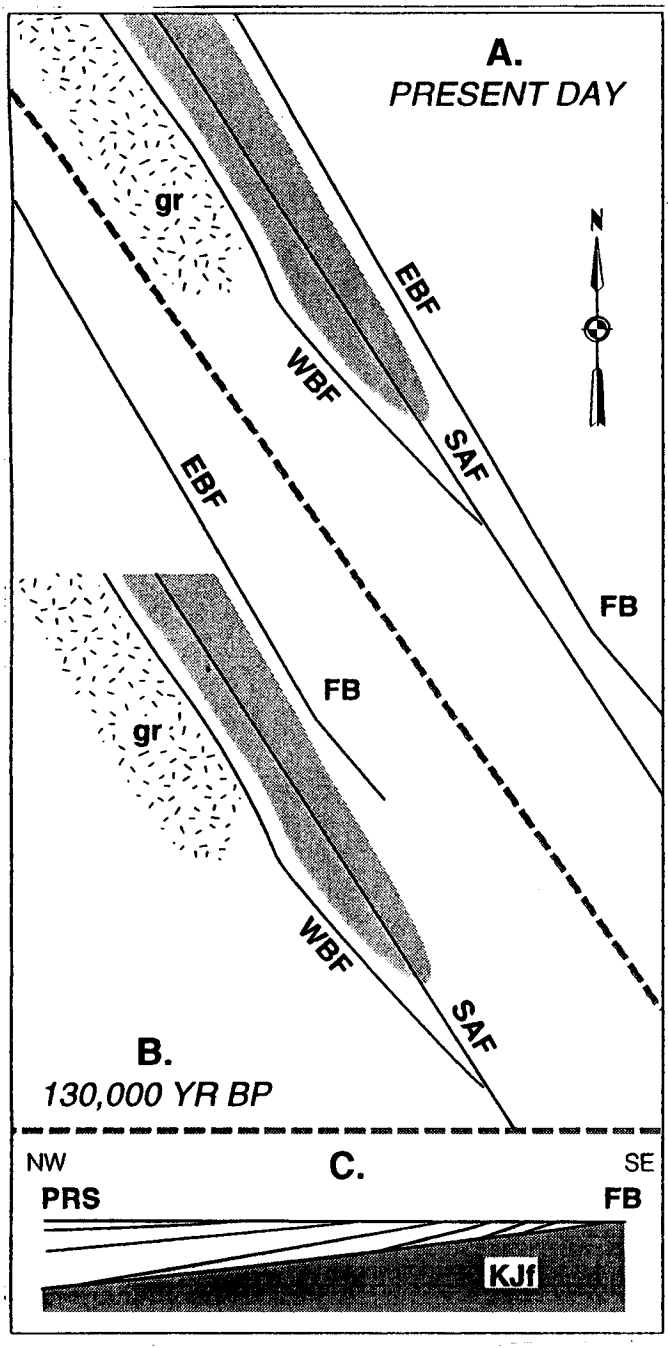

Figure 21. Possible mechanism for subsidence during OCF time and subsequent contraction and uplift. A.) Present-day geometry of the SAF (1906 trace), eastern boundary fault (EBF), and western boundary fault (WBF). From Galloway (1977). FB=Five Brooks; gr=Salinian granitic exposure; shaded area=depositional basin. With present geometry, contraction is occurring near Five Brooks and extension is occurring where fault strands diverge toward the northwest. B.) Geometry 130 ka with granitic exposure slid 6 km to the southeast to undo right-lateral SAF motions. C.) Profile along the fault valley to show shingling and progressive younging of sediments toward the northwest. PRS=Point Reyes Station; KJf=Franciscan basement.

(1994) found evidence of extensive alluvial fan deposition about 115–100 ka, after sea level had already started to fall from its highstand position. In summary, the accumulation of over 170 m of littoral sediment indicates that tectonic subsidence was a factor, but the influence of sea-level changes will remain uncertain until the duration of sedimentation can be further resolved.

Valley Deformation

There is evidence that the depocenter for OCF sediments has migrated northward and that the formerly subsiding basin has been subsequently compressed and uplifted. Sediments at the surface within the SAF valley between Five Brooks and Tomales Bay progressively young to the north, from basement exposures at Five Brooks, through Pleistocene deposits of the OCF and older alluvium (Qoa), to Holocene younger alluvium (Qal) and bay mud (Fig. 21C). Stratal deformation is most intense in the south; in the OCF, sediments dip steeply in the southern end of the outcrop belt near Five Brooks and dip gently in the north end, where they are overlain by younger alluvium. OCF estuarine mud, which was deposited near sea level, is now exposed at 60-m elevation near Five Brooks (locality I, Fig. 4; note that stage 5e sea level was higher than the present level, but only by 6 m, see Fig. 17). Further north, these littoral sediments have been buried beneath 35 m of alluvium at the P.M. No. 1 well location (Fig. 2), where OCF-like sediments extend to a depth of 300 m (California Oil and Gas, 1992; Fig. 6).

The gradual decrease in structural dip toward the north suggests that a depocenter located in the southern part of the outcrop belt migrated northward and that the sediment deposited in the south was beginning to be deformed while other sediment was being deposited further north. Thus, the measured 170-m (minimum) thickness of the OCF does not imply a basin over 170-m deep. Rather, strata may be shingled in a northerly-offlapping stack along the length of the outcrop belt, where layers become younger toward the northern depocenter, and Pleistocene sediments are overlapped by younger alluvium and bay mud deposits (Fig. 21C). This configuration is similar to the geometry of other basins adjacent to strike-slip faults (e.g., Ridge Basin, see Sylvester, 1988). Temporal and spatial alternations between subsidence and uplift are common along strike-slip fault systems, where crustal blocks are alternately squeezed upward in transpression or dropped downward in transtension (Sylvester, 1988).

The geometry of fault strands within the SAF valley now seems to be creating an area of contraction near Five Brooks and an area of extension near the south end of Tomales Bay. There are many areas of *minor*

subsidence and uplift along the SAF zone that are the result of small-scale fault bends and stepovers. However, the 1906 break within the SAF zone has a remarkably straight trace on the landscape, and there are no visible large-scale bends or stepovers that would produce *major* areas of extension or contraction. The overall fault valley, however, narrows near Five Brooks and widens toward the northwest (Fig. 2), a shape that reflects the location of faults other than the 1906 break (e.g., the eastern and western boundary faults). There is no historical movement known for these faults, but their clear topographic expression strongly suggests Holocene activity. Presently, the narrow width between valley-bounding faults at Five Brooks has created a constricting geometry that is compressing the sedimentary sequence and uplifting basement rocks to the surface. Further north, where valley-bounding faults diverge, fault motions have created a basin near the head of Tomales Bay, where sediments are accumulating. If this fault geometry is maintained, locations within the valley are first extended and then compressed as the Point Reyes Peninsula travels northwestward (Fig. 21).

Because sediments in the OCF were derived from a granitic source area, it is possible to use the present position of granitic basement rock on Inverness Ridge to estimate a long-term (past 125,000 yr) slip rate along the SAF zone. Assuming a north-flowing drainage (supported by paleocurrent measurements, Fig. 15), we restored the granitic mass to a position adjacent to the OCF outcrop belt. Moving the south end of the granitic outcrop belt to the south end of the OCF outcrop belt implies minimum post-depositional right-lateral offset of 5.8 km (Figs. 2 and 21). Assuming an OCF age of 130,000 yr (supported by TL dating), we obtain an estimated minimum slip rate of 45 mm/yr, nearly double the estimate of Niemi and Hall (1992) for movement during the past 2,000 yr along the 1906 trace of the SAF. Our longer-term rate applies to movements along both the San Gregorio and SAF systems but does not include possible movements along the eastern boundary fault, which is east of the OCF outcrop belt. Neither does our analysis evaluate the amount of vertical motions, suggested by stacked terraces along the valley sides of both Bolinas and Inverness Ridges, that may be uplifting the ridges relative to the valley floor.

CONCLUDING REMARKS

Olema Creek Formation sediments, which are exposed in a small part of the San Andreas fault valley south of Tomales Bay, reveal an interesting chapter in the geologic history of the region. Continued investigations will further refine our understanding of fault behavior and the role of climatic fluctuations as an influence on sedimentary processes.

ACKNOWLEDGEMENTS

We thank Lisa White for use of her micropaleontology laboratory and help with diatom identifications; Patrick Kociolek for access to California Academy of Science collections and help with diatom identifications; Charles Bickel, for help with mineral identifications; and Roger Byrne and Eric Edland, for assistance with pollen identifications. A review by Anna Buising improved the manuscript. Thanks to Tina Niemi, who introduced K Grove to the Olema Creek Formation, and to the National Park Service and the Boyd Stewart Ranch, who granted permission to explore and collect sediment in the area between Olema and Five Brooks. Acknowledgement is made to the Donors of the Petroleum Research Fund, administered by the American Chemical Society, for the support of this research.

REFERENCES CITED

Anima, R.J., Bick, J.L., and Clifton, H.E., 1988, Sedimentologic consequences of the storm in Tomales Bay, *in* Ellen, S.D., and Wieczorek, G.F., eds., Landslides, floods, and marine effects of the storm of January 3–5, 1982, in the San Francisco Bay region, California: U.S. Geological Survey Professional Paper 1434, p. 283–310.

Aydin, A., and Page, B.M., 1984, Diverse Pliocene–Quaternary tectonics in a transform environment, San Francisco Bay region, California: Geological Society of America Bulletin, v. 95, p. 1303–1317.

Blake, M.C., Bartow, J.A., Frizzell, V.A., Schlocker, J., Sorg, D., Wentworth, C.M., and Wright, R.H., 1974, Preliminary geologic map of Marin and San Francisco Counties and parts of Alameda, Contra Costa, and Sonoma Counties, California: U.S. Geological Survey, Miscellaneous Field Studies Map MF-574.

Bloom, A.L., and Yonekura, N., 1985, Coastal terraces generated by sea level change and tectonic uplift, *in* Woldenberg, M.J., ed., Models in Geomorphology: Winchester, Mass., Allen and Unwin, Inc., p. 139–154.

California Division of Oil and Gas, 1992, Regional Wildcat Map W6-4 (Lake, Marin, Mendocino, Solano, Contra Costa, Napa, and Sonoma Counties): Sacramento, California Divison of Oil and Gas, 1 sheet, scale approximately 1:125,000.

Chappell, J., and Shackleton, N.J., 1986, Oxygen isotopes and sea level: Nature, v. 324, p. 137–140.

Clark, J.C., Brabb, E.E., Greene, H.G., and Ross, D.C., 1984, Geology of the Point Reyes Peninsula and implications for San Gregorio fault history, *in* Crouch, J.K., and Bachman, S.B., eds., Tectonics and sedimentation along the California margin: Bakersfield, California, Pacific Section, Society for Sedimentary Geology (SEPM), p. 67–86.

Daetwyler, C.C., 1966, Marine geology of Tomales Bay, central California: Scripps Institution of Oceanography and Pacific Marine Station Research Report No. 6, 169 p.

Fairbanks, R.G., 1989, A 17,000-year glacio-eustatic sea level record: influence of glacial melting rates on the Younger Dryas event and deep ocean circulation: Nature, v. 342, p. 637–647.

Fletcher, C.H., Knebel, H., and Kraft, J.C., 1990, Holocene evolution of an estuarine coast and tidal wetlands: Geological Society of America Bulletin, v. 102, p. 283–297.

Galloway, A.J., 1977, Geology of the Point Reyes Peninsula, Marin County, California: California Division of Mines and Geology Bulletin 202, 72 p.

Hall, N.T., and Hughes, D.A., 1980, Quaternary geology of the San Andreas fault zone at Point Reyes National Seashore, Marin County, California, *in* Streitz, R., and Sherburne, R., eds., Studies of the San Andreas fault zone in northern California: Sacramento, California, California Division of Mines and Geology Special Report 140, p. 71–90.

Irwin, W.P., 1990, Geology and plate-tectonic development, *in* The San Andreas fault system, California: U.S. Geological Survey Professional Paper 1515, p. 61–80.

Kelsey, H.M., and Bockheim, J.G., 1994, Coastal landscape evolution as a function of eustasy and surface uplift rate, Cascadia margin, southern Oregon: Geological Society of America Bulletin, v. 106, p. 840–854.

Kennedy, G.L., Lajoie, K.R., and Wehmiller, J.F., 1982, Aminostratigraphy and faunal correlations of late Quaternary marine terraces, Pacific Coast, USA: Nature, v. 299, p. 545–547.

Klein, G. deV., 1985, Intertidal flats and intertidal sand bodies, *in* Davis, R.A., ed., Coastal Sedimentary Environments: New York, Springer-Verlag, p. 187–224.

Laws, R.A., 1988, Diatoms (Bacillariophyceae) from surface sediments in the San Francisco Bay: Proceedings of the California Academy of Sciences, v. 45, n. 9, p. 133–254.

Lawson, A.C., ed., 1908, The California earthquake of April 18, 1906: Report of the State Earthquake Investigation Commission: Washington, D.C., Carnegie Institute of Washington Publication 87, 451 p.

Li, W.-X., Lundberg, J., Dickin, A.P., Ford, D.C., Schwarcz, H.P., McNutt, R., and Williams, D., 1989, High-precision mass spectrometric uranium-series dating of cave deposits and implications for paleoclimate studies: Nature, v. 339, p. 534–536.

Nichols, M.M., and Biggs, R.B., 1985, Estuaries, *in* Davis, R.A., ed., Coastal Sedimentary Environments: New York, Springer-Verlag, p. 77-186.

Niemi, T.M., 1992, Late Holocene slip rate, prehistoric earthquakes, and Quaternary neotectonics of the northern San Andreas fault, Marin county, California: Ph.D dissertation, Stanford, California, Stanford University, 199 p.

Niemi, T.M., and Hall, N.T., 1992, Late Holocene slip rate and recurrence of great earthquakes on the San Andreas fault in northern California: Geology, v. 20, p. 195–198.

Quinn, B.B., and Grove, K., 1994, High-resolution gravity survey of subsurface morphology along the San Andreas fault north of San Francisco, California: EOS, v. 75, n. 44, p. 684.

Reneau, S.L., Dietrich, W.E., Donahue, D.J., Jull, A.J.T., and Rubin, M., 1990, Late Quaternary history of colluvial deposition and erosion in hollows, central California Coast Ranges: Geological Society of America Bulleitn, v. 102, p. 969–982.

Sarna-Wojcicki, A.M., Meyer, C.E., Adam. D.P., and Sims, J.D., 1988, Correlation and age estimates of ash beds in Late Quaternary sediments of Clear Lake, California, *in* Sims, J.D., ed., Late Quaternary climate, tectonism, and sedimentation in Clear Lake, northern California Coast Ranges: Geological Society of America Special Paper 214, p. 141–150.